Application of microbially induced calcite precipitation in erosion mitigation and stabilization of sandy soil foreshore slopes: A Preliminary Investigation

Emmanuel Salifu [a,c], Erica MacLachlan [a], Kannan Iyer [a,b], Charles W. Knapp [a], Alessandro Tarantino [a]

[a] Department of Civil & Environmental Engineering, University of Strathclyde, Glasgow, UK

[b] Department of Civil Engineering, Indian Institute of Technology-Bombay, Mumbai, India

[c] Present and Corresponding Address:
Emmanuel Salifu
Department of Agricultural and Environmental Engineering, University of Agriculture, PMB 2373, Makurdi, Nigeria.
emmy_salifu@yahoo.com.
+234 813 774 0504

Accepted for publication:
Engineeering Geology
27 December 2015

Abstract

Eroding foreshores endanger the floodplains of many estuaries, as such, effective and environmentally friendly interventions are sought to stabilise slopes and mitigate erosion. As a step in forestalling these losses, we developed laboratory microcosms to simulate tidal cycles and examined the mechanisms of erosion and failure on sandy foreshore slopes. As an experimental aim, we applied microbially induced calcite precipitation (MICP) to selected slopes and compared the effectiveness of this microbial geo-technological strategy to mitigate erosion and stabilise slopes.

To assess shoreline stability, thirty cycles of slowly simulated tidal currents were applied to a sandy slope. Significant sediment detachment occurred as tides moved up the slope surface. For steeper slopes, one tidal event was sufficient to cause collapse of the slopes to the soil's angle of repose (~35°). Subsequent tidal cycles gradually eroded surface sediments further reducing slope angle (on an average 0.2° per tidal event). These mechanisms were similar for all slopes irrespective of initial slope inclination.

MICP was evaluated as a remedial measure by treating a steep slope of 53° and an erosion-prone slope angle of 35° with Sporosarcina pasteurii and cementation solution (0.7 M $CaCl_2$ and urea) before tidal simulations. MICP produced 120 kg calcite per m^3 of soil, filling 9.9% of pore space. Cemented sand withstood up to 470 kPa unconfined compressive stress and showed significantly improved slope stability; both slopes showed negligible sediment erosion. With efforts towards optimisation for upscaling and further environmental considerations (including effect of slope saturation on MICP treatment, saline water and estuarine/coastal ecology amongst others), the MICP process demonstrates promise to protect foreshore slope sites.

Keywords: MICP, slope stabilization, erosion mitigation, foreshore, rip current.

Highlights

- Untreated and treated sandy slopes were subjected to tidal currents in a microcosm
- Untreated slopes fell to angle of repose, eroding 0.2° slope angle per tidal event
- MICP treatment was with S. pasteurii and solutions of urea and calcium;
- Significant cementation was achieved with calcite filling 9.9% pore space.
- MICP-treatment stabilised slopes resulting in negligible erosion.

1.0 Introduction

The erosion of foreshore slopes by rip currents and associated tidal flows represents a major problem in many estuarine environments (Short, 1985; Winn et al., 2003). For example, erosion threatens the bank defences that protect >90,000 ha of arable land and 30,000 people with property within the flood plain of the Humber estuary in the UK (Winn et al. 2003). Another possible implication of the foreshore erosion is the loss of intertidal habitat due to the phenomenon of 'coastal squeeze' or decrease in spatial extent of intertidal areas over time (Fujii and Raffaelli, 2008).

Typical rip current events take place for less than 20 seconds at 3 - 4 hours intervals, with velocities of up to 1 $m \cdot s^{-1}$ (Short and Brander, 1999; MacMahan et al., 2006; Scot et al., 2009; Haller et al., 2014). Consequential slope failure and erosion from these tidal currents remain a geotechnical challenge in most coastal and estuarine environments. Foreshores (see Fig.1), whether coastal or estuarine, are gradually washed away as they undergo erosion mechanisms due to constant exposure to tidal currents. Mechanisms of coastal and/or estuarine foreshore erosion under tidal currents have not been fully elucidated in literature. Even though coastal shorelines differ from estuarine environments in terms of geology and intensity of tidal events experienced (Sharples, 2006), it may be worthwhile to borrow the already established concept of erosion mechanisms on coastal shoreface as a starting point to hypothesize if expectedly similar erosion mechanisms may occur on estuarine foreshores. Erosion on coastal shoreface involves gradual detachment and transport of soil grains down the slope surface during the up-rush phase of tidal currents; it is then deposited on the slope surface or foot of the slope upon tidal back-wash. Some sediment may be transported away from the area of detachment. Depending on the velocity of the tidal currents and the ease of detachment of soil grains, erosion can occur quickly and consequentially leads to loss of entire shores and increased incidences of flood in coastal flood plains (Conley and Inman, 1994; Cox et al., 1998; Petti and Longo, 2001; Elfrink and Baldock, 2002; Longo et al., 2002; Cowen et al., 2003; Conley and Griffin, 2004; Masselink et al., 2005).

Studies reported in the literature have identified soil properties such as clay content, microbial activity, bulk density and moisture content as factors that affect coastal or hillslope erosion (Amos et al. 1996; Fang and Wang, 2000; Fang et al., 2013); by extension, it would be reasonable to add that these factors and others like shore slope angles, tidal effects and nature of available vegetative cover may also play key roles in estuarine foreshore erosion.

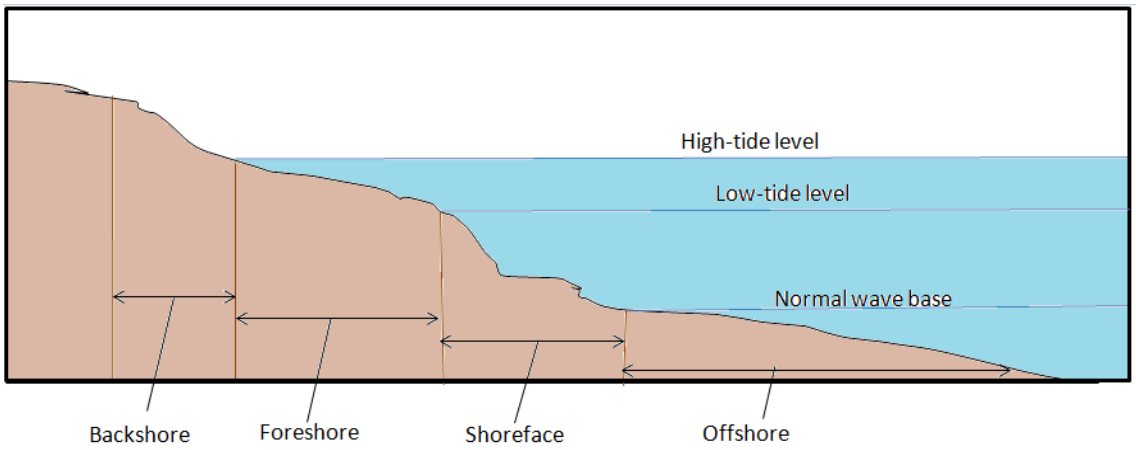

Fig.1: **Typical coastal/estuary anatomy showing foreshore, tide levels and other shores**

Considering the above erosion mechanisms and factors that interplay in shore erosion, it therefore follows that a potential strategy to effectively control estuarine foreshore erosion would be one that is designed around these factors and supposed erosion mechanisms. Effective stabilisation technique for foreshore slopes remains a challenge, and there are no approaches proposed in existing literature to prevent foreshore erosion with minimal implications. If one were to think about remedial measures for foreshore slope erosion, one may approach these by borrowing techniques that are currently adopted in general erosion control strategies; these may be by applying techniques that support the slopes in any of the following two ways: 1) by using foreign soil improvement material, e.g., use of membrane structures for soil reinforcement (Liu and Li, 2003), chemical cementation using cement, fly ash, lime or inorganic polymer stabilizers (Liu et al., 2011); or 2) by simply improving the in-situ soil properties through the application of the 'biogenic/microbial methods' (Agassi and Ben, 1992; Dejong et al., 2013). However, there are limitations to some of these techniques.

Foreign materials like geotextiles, wire meshes, cable nets, nails or sheets and other membrane structures physically installed to promote slope enforcement do not modify soil properties (Singh, 2010); they are often expensive and require machinery that may disturb infrastructure (van Paassen et al., 2009); and they also affect plant growth. Chemical/organic stabilizing agents, apart from being ecologically unfriendly in some cases, may fail when applied to soils subject to constant wet conditions such as coastal shores; there is also the challenge of stabilizers having high viscosity or hardening too fast, and therefore being unsuitable for application in large areas (van Paassen et al., 2009).

Based on these submissions, therefore, a more formidable remedial technique suitable for estuarine foreshore slope erosion might be the biogenic/microbial approach for soil property improvement. This is the premise, on which the current trend of microbial geotechnology to improve soil properties, has developed. This technology has shown superlative efficiency and effectiveness in improving soil properties with ease and less cost, and it enhances environmental sustainability (Dejong et al., 2013).

One type of microbial geotechnology based technique adapted for soil stabilization is microbially induced calcite precipitation (MICP), where microorganisms of the Bacillus genus (e.g., alkaliphilic Sporosarcina pasteurii) induce calcite precipitation through the hydrolysis of urea in the presence of dissolved calcium salt solution, organic carbon and optimum environmental conditions (pH 7-9, temperature 27-30°C) (Mitchell & Santamarina 2005; Van Paassen et al. 2007; Whiffin et al., 2007; Harkes et al., 2008; Ivanov and Chu, 2008; van Paassen et al., 2009; DeJong et al., 2009).

The application of the MICP techniques for stabilizing foreshore slopes still remains a budding line of research. Meanwhile, laboratory investigations to understand soil erosion processes have been reported in the literature, but little has been done regarding coastal foreshore slopes. The closest investigations, linking laboratory studies of water-induced soil erosion and/or stabilization to MICP treatment, were done by Van Paassen et al. (2010) and Esnault-Filet et al.

(2012). Even though their work involved treatment of saturated soils, it did not consider soils at slopes, their erosion mechanism, nor the effects of intermittent tidal currents on soil slopes. Here, the experimental laboratory-scale microcosms aim to demonstrate slope failure and erosion mechanisms on soil slopes as tidal processes occur and to test the potential effectiveness of MICP in stabilizing such slopes and mitigating slope surface erosion. This microcosm approach is an advantageous preliminary step, which provides an experimental approach at laboratory scale, where environmental factors can be controlled, and scaled down models of actual soil slopes could be investigated. Subsequently, other complex variables may be introduced as a build-up towards large-scale field implementation of findings.

1.1 Background

MICP biochemistry is well documented in literature (Ferris et al., 1996; Mitchell et al., 2010). It involves urea hydrolysis:

$$CO(NH_2)_2 + 2H_2O \rightarrow 2NH_3 + H_2CO_3^{2-} \quad \ldots\ldots (1)$$

Ammonia in the presence of water forms ammonium and hydroxyl ions, which increases ambient pH around the bacterial environment to about 9 (equation (2)) (Dejong et al., 2006; Van Paasen, 2009), and the resultant alkaline environment shifts the carbonate systems to ultimately producing more carbonate ions (equations (3-4)):

$$2NH_3 + H_2O \leftrightarrow 2NH_4 + 2OH^- \quad \ldots\ldots (2)$$

$$H_2CO_3 + 2OH^- \leftrightarrow HCO_3^- + H_2O + OH^- \quad \ldots\ldots (3)$$

$$HCO_3^- + H_2O + OH^- \leftrightarrow CO_3^{2-} + 2H_2O \quad \ldots\ldots (4)$$

The carbonate reacts with calcium ions, forming calcium carbonate, or calcite crystals, as follows:

$$Ca^{2+} + CO_3^{2-} \rightarrow CaCO_{3(s)} \quad \ldots\ldots (5)$$

Calcite crystals serve as the 'cementing bridges,' which bind soil grains together, and they have been found to be highly effective in binding soil particles up to 50 years and improving their geotechnical properties, such as shear strength (DeJong et al., 2009). Cementation, whether obtained from bio-cementation or bio-clogging, depend on several factors, such as: 1) bacterial aggregation (El Mountassir et al., 2014); 2) the composition and concentration of soluble calcium (Harkes et al., 2010); 3) pore size distribution of the media; 4) application strategy of bacteria (e.g. one pore volume) and salt (e.g. two pore volumes) to promote fixation, homogeneous distribution of bacteria and cementation yields (Harkes et al., 2010); 5) the injection rate into the soils (depending on the permeability of soil media); 6) the grouting technique and the duration at which specified volume is applied.

2.0 Material and methods

2.1 Materials

2.1.1 Microbial suspensions

Solutions of S. pasteurii were prepared from strain ATCC 11859, which have been stored in agar plates (comprised of Brain Heart Infusion (BHI) agar and 2% urea; see Table S2 for media composition), and grown overnight (BHI broth and 2% urea). Cells were harvested at late exponential phase, centrifuged (10 000 x g, 10 min) and diluted to final OD_{600} of 1.0 (equivalent to 3 x 10^8 colony forming units (CFU) mL^{-1} (El Mountassir et al., 2014)) at one pore volume to be treated. In both treatment cases, the BHI media were prepared with deionized water and autoclaved at 121°C for 20 minutes. Urea solutions were sterilely filtered (0.2 µm filter) into the broth. Media and inoculants were placed on a shaker table at 160 rpm for 24 hours during growth.

2.1.2 Cementation solution

A solution of 0.7 M $CaCl_2$ and urea served as fixation fluid and cementation fluid. This molar concentration was based on the recommendation of Harkes, et al. (2010) that solutions greater than 0.5 M $CaCl_2$ and urea are best suitable for cementation.

2.1.3 Perspex container

The process of simulating tidal cycles for determining soil slope erosion and the injection of treatment solutions into soil slopes were all carried out in a cube-shaped container (0.2m sides) made from 'Perspex' (polymethyl methacrylate, PMMA). PMMA is a tough, transparent, synthetic fibre plastic that serves as a good alternative for glass for applications in environmental and life science laboratory experiments (Uzunoglu et al., 2014) (see Figure 2). Silicone sealant was used to bind and seal the edges. One face was detached by simply using a sharp scalpel to separate the joints (this side was re-sealed with silicone sealant after soil was supplied into the box). This side of the container is fitted with a valve in the outward end and a wire mesh to distribute flow in its inward area. A pipe of 4 mm internal diameter was used to supply and drain water via the dual inlet-outlet valve. The water tank was positioned at height of 1.3 m above the base of the Perspex box. Three holes measuring 3 mm ϕ were made at the top of the container to help transfer air during the tidal cycles and, secondly, serve as ports for flexible plastic tubing during injection of treatment solution.

2.1.4 Soil

Sandy soil was sourced from Troon beach in Ayrshire, UK and air dried in the laboratory. Intrinsic and experimental test properties of the soil are given in Table 1 and Table 2, respectively, while the grain size distribution of the soil is shown in Figure S1 (supplemental figure).

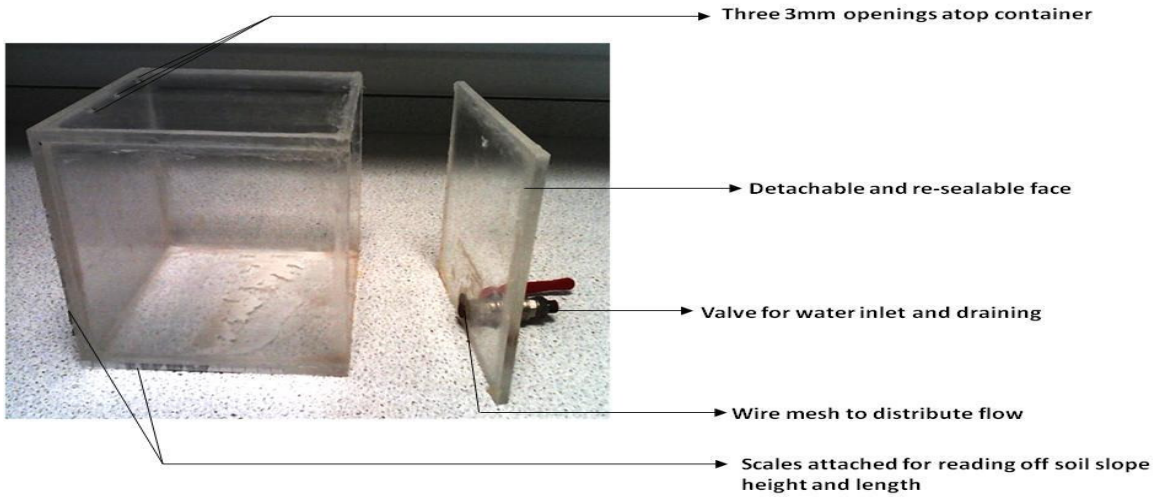

Figure 2: The Perspex box container. Cube shaped with each side equal to 200 mm.

Table 1: Intrinsic properties of the sandy soil.

Property	Value	Determination method
Saturated hydraulic conductivity, cm/sec	1.5×10^{-3}	Constant head method
Specific gravity	2.65	
Coarse sand percentage, %	0.6	
Medium sand percentage, %	31.9	
Fine sand percentage, %	67.5	ASTM D422-63e2 Standard methods for particle size analysis of soils
D_{60}, mm	0.4	
D_{30}, mm	0.3	
Effective size (D_{10}), mm	0.24	
Coefficient of curvature (C_c)	0.94	
Coefficient of uniformity (C_u)	1.67	
Classification	Uniformly graded sand	ASTM D2487-06e1 Standard Practice for Classification of Soils for Engineering Purposes (Unified Soil Classification System
Angle of repose (oven-dried sample)	28.5	Miura et al., 1997
Angle of repose (wet)	35.7	

Table 2: Properties of the packed soil in the experiments.

Property	Value	Remarks
Bulk density (g cm^{-3})	1.82 - 1.89	This was achieved by pouring the required quantities of water and soil at specified moisture content into the Perspex box via the detachable face, and literally 'compacting' the wet sand using hands and spatula to fit into the slope expected, guided by the scale attached to the Perspex box.
Dry density (g cm^{-3})	1.47 - 1.50	
Porosity	0.44	
Initial Moisture content (%)	25.0	This moisture content was found sufficient to wet soil completely as if due to tidal effect, and also enough to prevent slope from collapsing by itself.
Slope angles (°)	35, 48, 51, 53	35° is the approx angle of repose for the wet sand; 53° was the steepest stable slope obtainable by compacting soil at 25 % moisture content for the experimental purposes

Soil samples were oven-dried at 105°C overnight to minimise interferences from antecedent microbial or plant communities. Quantity of soil needed and soil pore volumes were determined from the slope dimensions and bulk density. Computed pore volumes were used for determining volumes of bacterial and cementation solutions.

2.1.5 Water

To minimise any interplay of extraneous variables like salt concentrations in water and/or introduction of foreign bacteria species, water was purified by reverse osmosis. Also, the same purified water was used at intervals between application of bacterial solution and cementation fluids to avoid clogging.

2.2 Experimental set up/methodology

Two basic experimental set ups were developed for each assay. A schematic view of the first set up, which established the slope erosion mechanisms, is shown in Fig. 3a. The second set up, which was for the MICP treatment process, is as shown in Fig. 3b.

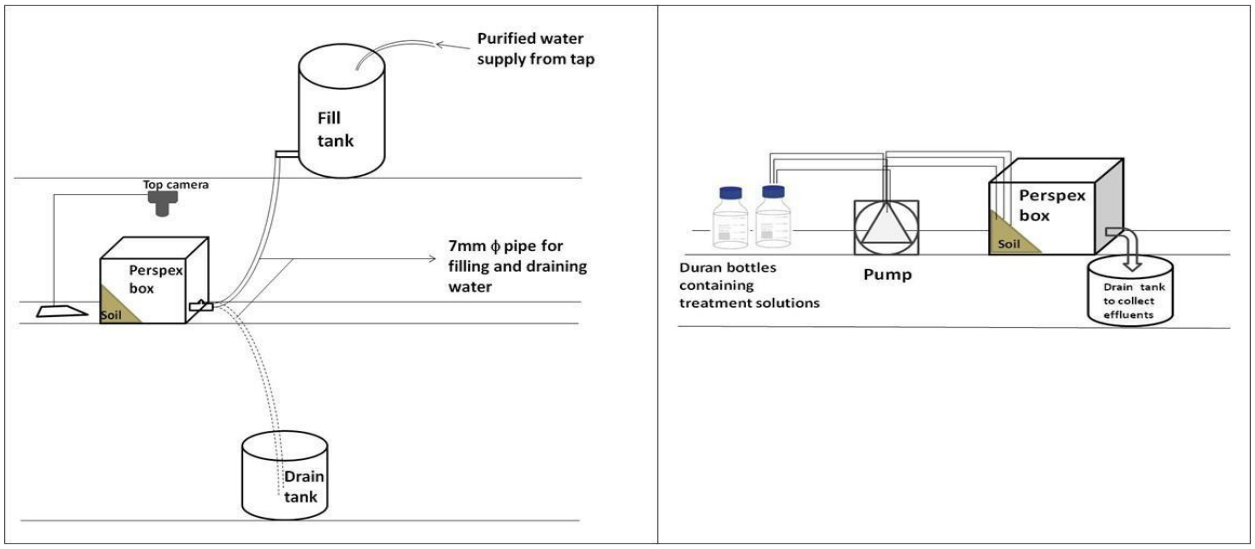

Figure 3. (a) Experimental set up for simulating the tidal current processes to determine slope erosion/failure mechanisms. (b) Experimental set up showing the MICP treatment process with permeation grouting. Flexible tubes were used to transfer treatment solutions via a pump into the soil. Effluents that flowed out were collected as shown.

The investigation involved two core workplans to achieve experimental objectives, these are: 1) simulation of tidal cycles without any cementation treatments, performed to establish baseline erosion mechanisms with three different slope conditions, i.e., 48°, 51° and 53°; and 2) simulation of tidal cycles on MICP-treated slopes. The microbial and cementation solutions necessary for slope treatments were prepared for two slope treatments: one for the steepest slope before collapse (53°, which is steeper than the angle of repose) and the second, representing the approximate slope formed immediately after steep slope collapsed (35°, erosion prone slope); it was after the collapse to this slope that progressive sediment erosion trends were observed and studied per tidal cycle. Other additional experimental procedures for determination of calcite

production and estimation of strength of cemented soil were, thereafter, carried out to determine treatment effectiveness. Specific details for each work plan are presented below.

2.2.1 Simulation of tidal cycles (on untreated and treated soils). Initial microcosm simulations established and evaluated slope failure at three different starting slopes (48°, 51°, and 53°). The prepared sand (section 2.1.4) was brought to a moisture content of 25.05% and formed into slopes at compacted bulk density of 1.82 -1.89 g/cm^3 in the Perspex container. After MICP treatment on two selected slopes (53°and 35°), another set of tidal simulations was performed to evaluate the effect of treatment on slope failure. Two cameras (Nikkon 360XLR and a webcam) were fitted on retort stands from the top and side of the box to monitor bank stability; video and still images were captured using 'Candy Labs VideoVelocity' software. The procedures for both tidal simulations (on the untreated and treated soil slopes) were same and carried out in the Perspex box as follows:

The uprush water flow came in at inflow rate of 10^{-5} m^3/s. The rising tide was allowed to fully saturate the slope with the water level submerging the slope crest by 0.08 m. As soon as the uprush got to the top of the slope, the valve was opened to allow the tide fall by draining water out of the Perspex box at 1.3 x 10^{-5} m^3/s. Backwash velocity was slightly higher than uprush because the slope head makes the rip current backwash faster than its upflow. Following the tidal cycle, the change in slope was noted by measuring the height and base of the soil slope in the Perspex box using the graduated scale attached to it. Sediments washing into the drain container were also collected, weighed and recorded at the end of every ten cycles. The mass of soil deposited at foot of slope was determined at the end of the thirtieth cycle. The tidal procedure was repeated thirty times and carried out for soil masses of 2250g, 1000g and 500g, forming slope angles of 48°, 51° and 53° respectively, as well as for the treated slopes of 53°and 35°. (The soil masses adopted were scaled down progressively to determine erosion mechanism at various soil quantities and to have minimum possible soil volume that effectively demonstrates erosion mechanisms and minimise the resources required for MICP).

2.2.2 Application and assessment of MICP technique. The procedures involved in injecting the microbial suspensions and cementation solutions (sections 2.1.1 and 2.1.2) into pre-selected sandy slopes (53°and 35°), and some complementary tests or ancillary investigations carried out to assess/quantify effectiveness of treatment and quality of cementation on the two treated soil slopes are detailed as follows:

Injection of bacterial solution and cementation solution into the soil. Air dried soil samples were collected, autoclaved and weighed. The soil mass used, moisture content and compacted bulk density for both slopes treated are given in Table 3.

Table 3 : Masses, moisture content, volumes and bulk densities of treated slopes

Slope angle treated	Slope dimension (cm) and ratio	Mass of autoclaved soil (g)	Moisture content (%)	Volume of soil (cm^3)	Compacted bulk density (g/cm^3)
35°	4.8/6.9 (1:1.44)	500	25.05	331.2	1.89
53°	8/6 (1:0.75)	700	25.05	480.0	1.82

After compacting the soil to desired bulk density in the Perspex box, three grout pipes (flexible plastic straws) were used per slope treatment to disperse cementation solutions. The length of the straws was randomly perforated using a pin, and the bottom of each straw was plugged with silicone sealant. These were then installed through the openings atop the Perspex box into the soil. The peristaltic pump was calibrated to apply the solutions at 6 mL/min, as advised by Whiffin et al. (2007). To induce calcite precipitation by grouting, the pores of sandy soil slopes were treated by application of one pore volume of S. pasteurii suspension and two pore volumes of 0.7 M $CaCl_2$ and urea (fixation/cementation) solution, sequentially. The bacteria solution was first pumped in, and thereafter, the conduits (tubes) were flushed with de-ionized water for about 5 minutes to avoid clogging. After this interval, the cementation solution was then injected into the soil. This entire process represents one treatment cycle. Multiple injection of bacterial

solution is adopted here as recommended by El Mountassir et al. (2014) to forestall the possibility of microbial incapacitation due to encasement in calcite as reported by Cuthbert et al. (2012) and Tobler et al. (2012). Based on pore volumes, 150mL and 220mL suspension solutions of S. pasteurii were applied to soil slopes of 35° and 53°, respectively. S. pasteurii strain ATCC 1187 were aseptically cultured on BHI (Table S.1 for media composition) agar plates with 2% w/v urea for one week at 21°C, and then stored at 4°C for short-term storage. To prepare solutions for each treatment cycle, the microorganisms were harvested from the plates and aseptically inoculated into BHI broth with 2% urea at pH of 7.4 (based on El Mountassir, et al. 2014). Fresh solutions were prepared daily.

Eighteen cycles of MICP treatment solutions (3 times per day, for 6 days) were pumped via tubing to soil slopes (35° and 53°). One-hour interval was allowed in between treatment cycles to enable the reactions to completely take place in the soil before another cycle begins. The adoption of eighteen treatment cycles over six days was based oral communication with El-Mountassir and McLachlan (2014).

Effectiveness of treatment on slope stability and erosion mitigation. MICP-treatment efficacy was tested by subjecting slopes to simulated tidal currents. At the end of the eighteen treatment cycles, thirty tidal current cycles were simulated on each of the two treated slopes (Section 2.2.1); slope changes were noted, to compare with changes in untreated slopes subjected to same tidal events.

Determination of amount of calcite production. Effluent solution were collected from the foot of the soil slope with a 20-mL syringe during the treatment cycles, and filtered through a 0.42-µm sterile filter to remove bacteria. Sample collections were done at exactly five minutes after the 4^{th}, 7^{th}, 9^{th}, 11^{th} and 13^{th} treatment cycles, and were frozen in plastic centrifuge tubes at -20°C. This entire sampling process was conducted within 1-2 minutes to minimise post-sampling and pre-storage chemical reactions.

Effluent ammonium and calcium concentrations were determined using colorimetric KONE analyser and Inductively Coupled Plasma Optical Emission Spectrometry (ICP-OES),

respectively, at the Strathclyde Eco-Innovation Unit (SEIU) at University of Strathclyde. Samples were diluted 1:200 mL and 1:500 mL, respectively, for detection limits. Ammonia represented reaction by-products, while the calcium concentrations represented unreacted reagent precursor.

Additionally at conclusion of MICP treatment and tidal cycles, the cemented soil slopes were removed from the Perspex box and oven dried; the oven dried mass was determined using the weighing scale, and then the sample was washed in 10% HCl to remove the calcite formed. The respective sample weights after acid washing and oven drying were recorded.

Estimation of effectiveness of the treatments versus amount of calcite formed. Strength of cemented soil was determined using unconfined compressive strength (triaxial) test machine (Wykeham Farrance, Tritech Model, 50kN capacity). Four core samples (two from the 53° slope and two from 35° slope) were collected and trimmed to frictionless smooth edges of height:diameter ratio of 1.2:1. The length and diameter of specimens to be tested were measured and recorded, and as much as possible, moisture loss was minimised in each specimen. Without applying confinement, the triaxial cell was placed on the sample. According to ASTM D2166-00 standards, rate of strain was computed at 1.27 mm min^{-1}. The test started by application of load and stopped when a drop in the stress-strain plot was observed.

3.0 Results and Discussion

3.1 Examination of slope stability - Experiments on untreated sand slopes: Thirty tidal cycles were simulated on three different slopes initially to establish slope failure and understand erosion mechanisms. Figure 4 shows the response or evolution of the slope for the three different initial inclinations of the slope during the first simulated tidal cycle.

Visual evidence showed that the first simulated rip current cycle caused a drastic collapse of the untreated slope in all three cases (48°, 51° and 53°); subsequently, gradual sediment erosion

continued, with slopes changing progressively from about 35° to approximately 29° in the remaining 29 cycles (Figures 4-5).

During the first tidal cycles, the force of the rising waters detached soil grains and circulated them in the path of the current. Most of them settled and rolled down the slope further destabilising other grains. Some grains deposited themselves at the foot of the slope, while others stopped and settled slightly lower than their original position. The first tidal cycle resulted in the development of a 'new' pseudo-slope beneath the saturated area as the tide moved upwards (Figure 4). As the upsurge of water surpassed midpoint of slope height, the entire soil mass above the waters collapsed. This instantly decreased slope height and increased slope length, a typical 'rotational' type slope failure. The backwash was not as eventful; there was further deposition of some fine particles in the tidal water as it receded along the slope surface. This process was similar for all three soil masses/slopes tested (Figure 5).

The new slope formed after the initial collapse due to tidal effect was approximately 35° in all three cases studied. This value is similar to the typical angle of repose measured for wet sandy soils (i.e. 35.71°). There were no significant differences between the trends of slope change per tidal cycle. The next 29 tidal cycles simulated showed gradual changes in the slope, which can be interpreted as progressive erosion of surface sediments leading to decreasing slope height and increasing slope length, albeit less drastic during these cycles compared to the first tidal cycle. Similar observations for saturated sandy soil slopes of different heights in this study (48° - 53°) justified the adoption of masses of 500g and 700g for forming slopes with corresponding slope angles of 35° and 53°, respectively, in the experiments for MICP treated slopes.

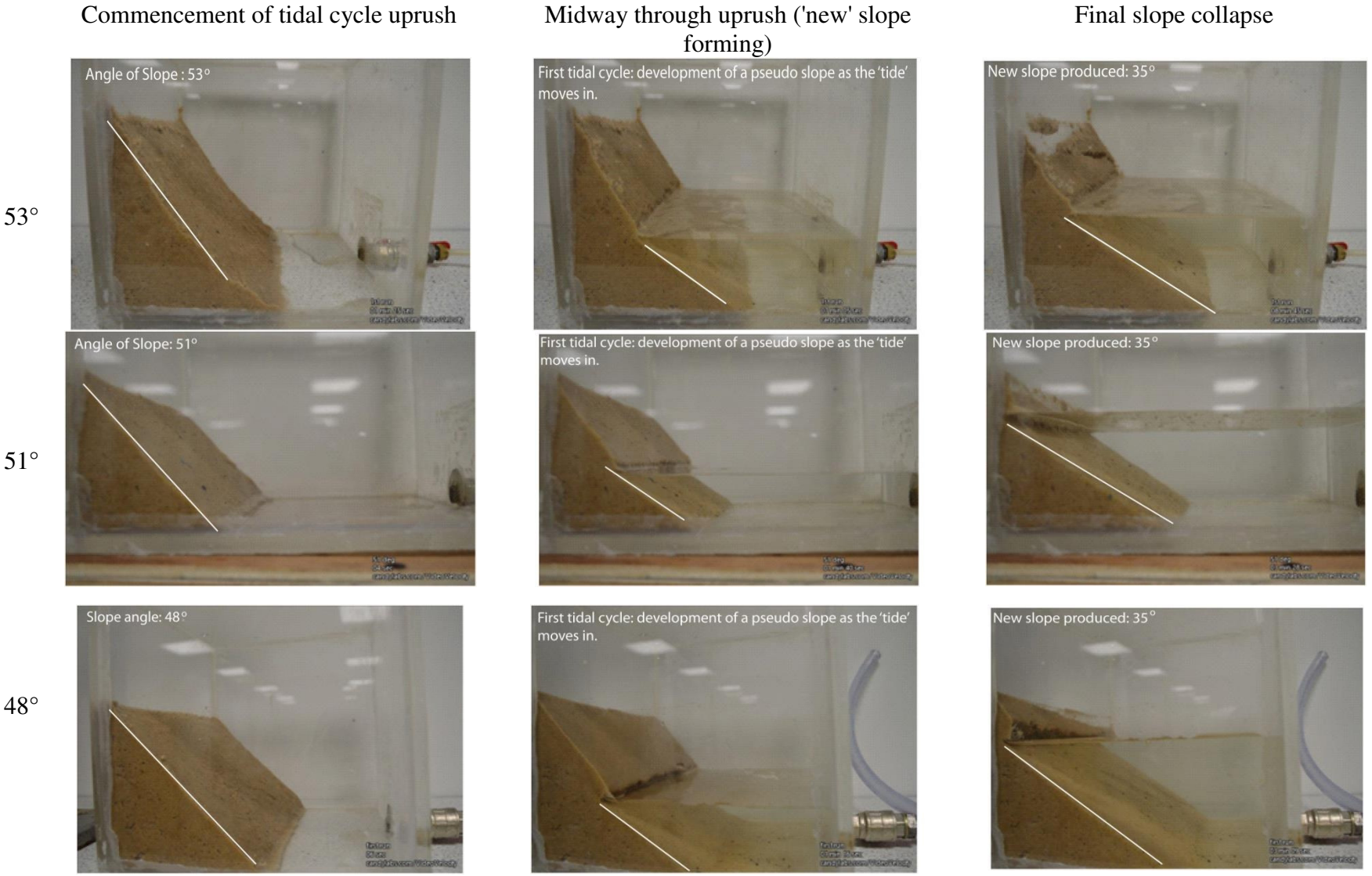

Figure 4: Slope collapse during first simulated tidal cycle uprush

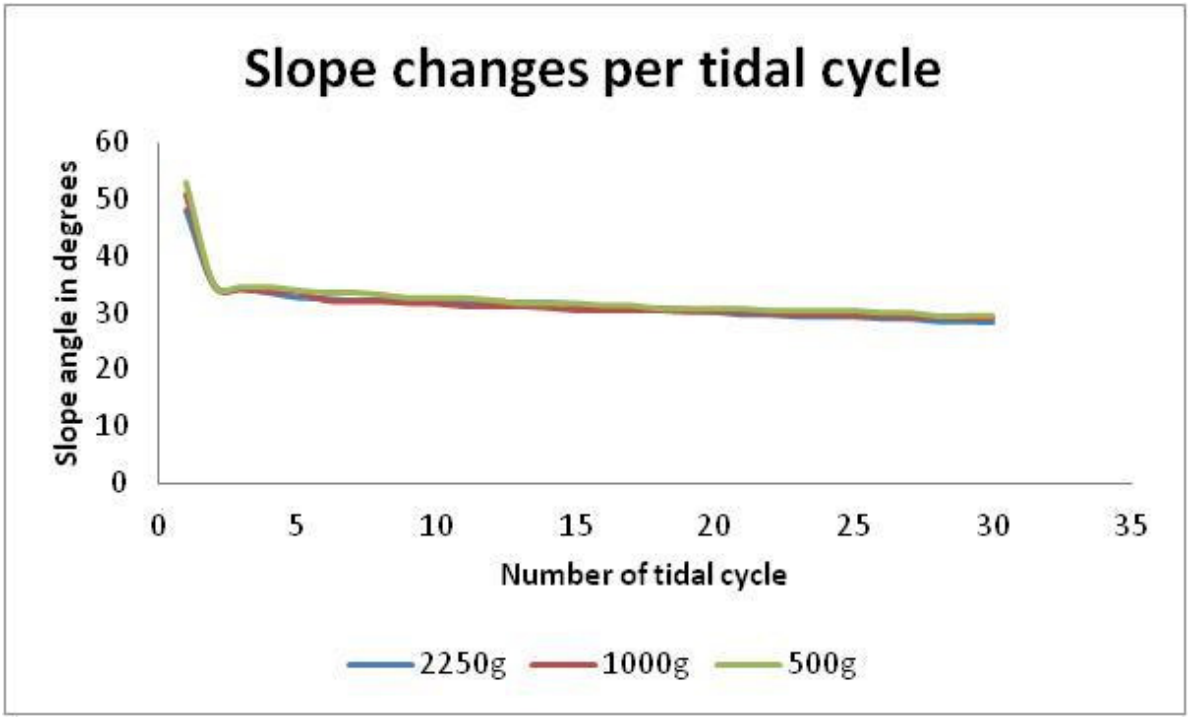

Figure 5: Changes in slope per tidal cycle simulated in all three soil masses (slope collapse and erosion phases)

The mechanism of slope failure was found to be similar for all three steep slopes tested (48°, 51° and 53°) even though they were made up of different respective soil masses of 2250g, 1000 g and 500 g; this indicates that sandy soil slope failure and erosion mechanisms follow similar trends irrespective of the soil mass forming the slope. Further studies may be necessary to substantiate whether this can be extended to other scenarios.

The trend of erosion occurring after sandy soil slope failure (due to effects of tidal currents) obeys the linear function in the range investigated. The findings of this report indicate that foreshore sandy slope angles may decrease by approximately 0.2° for each tidal current cycle that occurs on it. An extrapolation of this relationship would give a fair idea of when the loss of foreshore may occur subject to the respective number of tidal cycles (although apparent linear functions would eventually become asymptotic). This is a very fundamental finding and may require further investigations that would put several variables in context to predict this trend more accurately.

3. 2 Examination of slope stability - Experiments on treated sand slopes: At the end of the eighteen treatment cycles on each of the treated slopes (35° and 53°), thirty tidal current cycles were simulated under the same water flow rates and conditions as used to establish slope failure and erosion baselines (Section 2.2.1). This was done in order to make it easy to compare stability between untreated and treated slopes subjected to tidal processes. Figures 6-7 show slope failure and erosion occurrence for 53° and 35° slopes at selected tidal cycles in both untreated and treated slopes. Graphical plot of the results for treated slopes of 35° and 53° juxtaposed with untreated slopes (starting at the collapsed slope angle of 34.8°, where erosion began, and slope angle of 53°, slope of instability) are as represented in Figures 8-9.

In both cases with the MICP, visual evidence showed negligible changes in the slope angle per tidal cycle compared to what was obtained without treatment. Figures 6-7 emphasise the visual differences as water rose mid-way the height of treated and untreated slopes in 1st, 2nd, 20th and 30th tidal cycles. The quantity of sediment deposited at the floor of the Perspex box (foot of slope) visibly increased for untreated slopes per tidal cycle compared to the treated slopes.

Clearly, Figures 6-9 imply that there was marked improvement in the treated sandy slopes as it shows significant stability under the same tidal cycles that hitherto collapsed the untreated slopes. MICP was capable of stabilizing the sandy soil slopes and also mitigated the erosion of slope surface significantly. Broadly speaking, for an eroding/unstable sandy foreshore slope in estuarine or coastal environments, application of MICP could potentially be effective in cementing soil grains and thus mitigating slope failure or erosion to a reasonable extent.

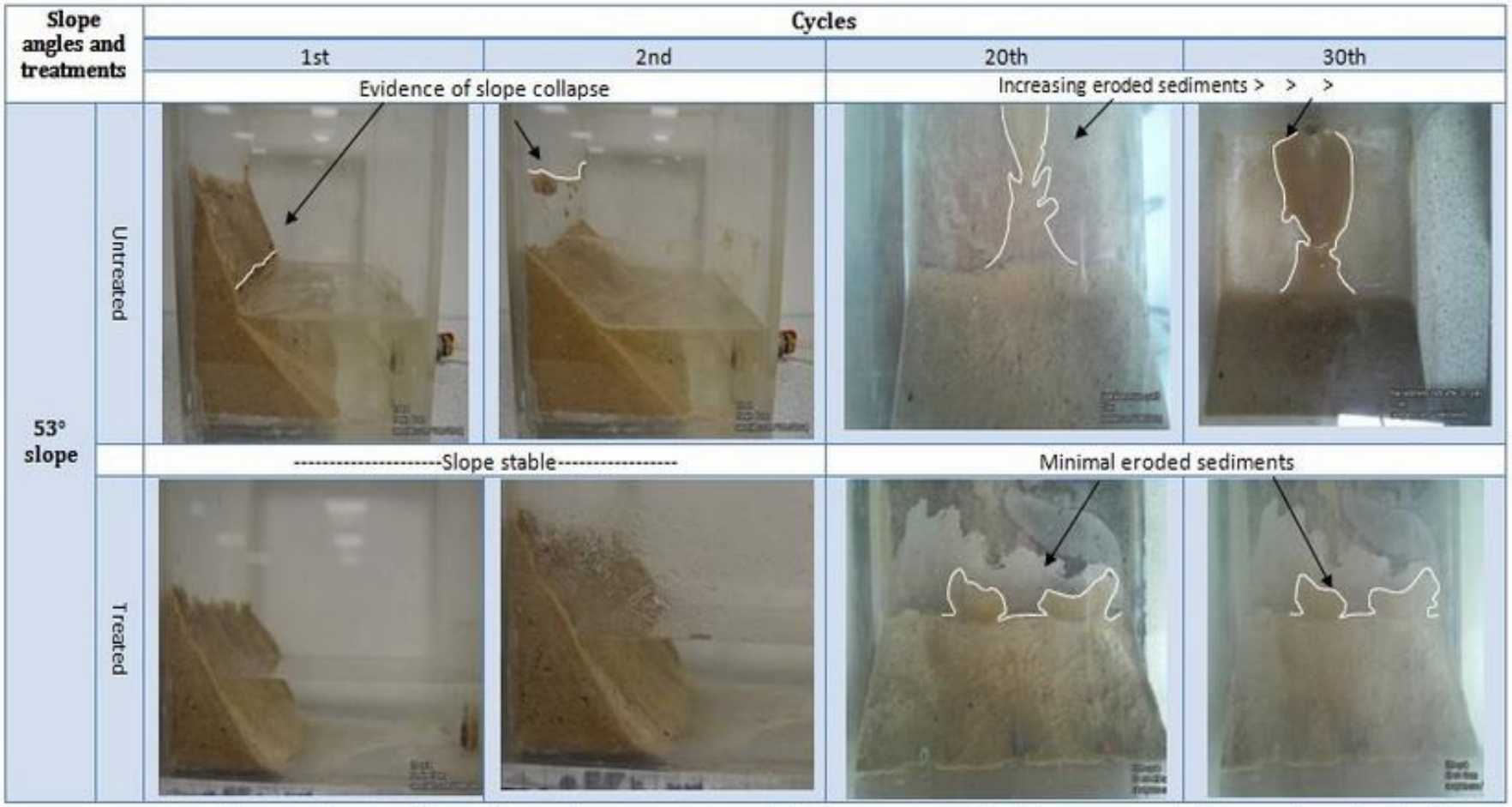

Figure 6. An array of images showing slope failure and erosion untreated 53° slope juxtaposed with MICP-treated slope at selected cycle of simulated tidal events.

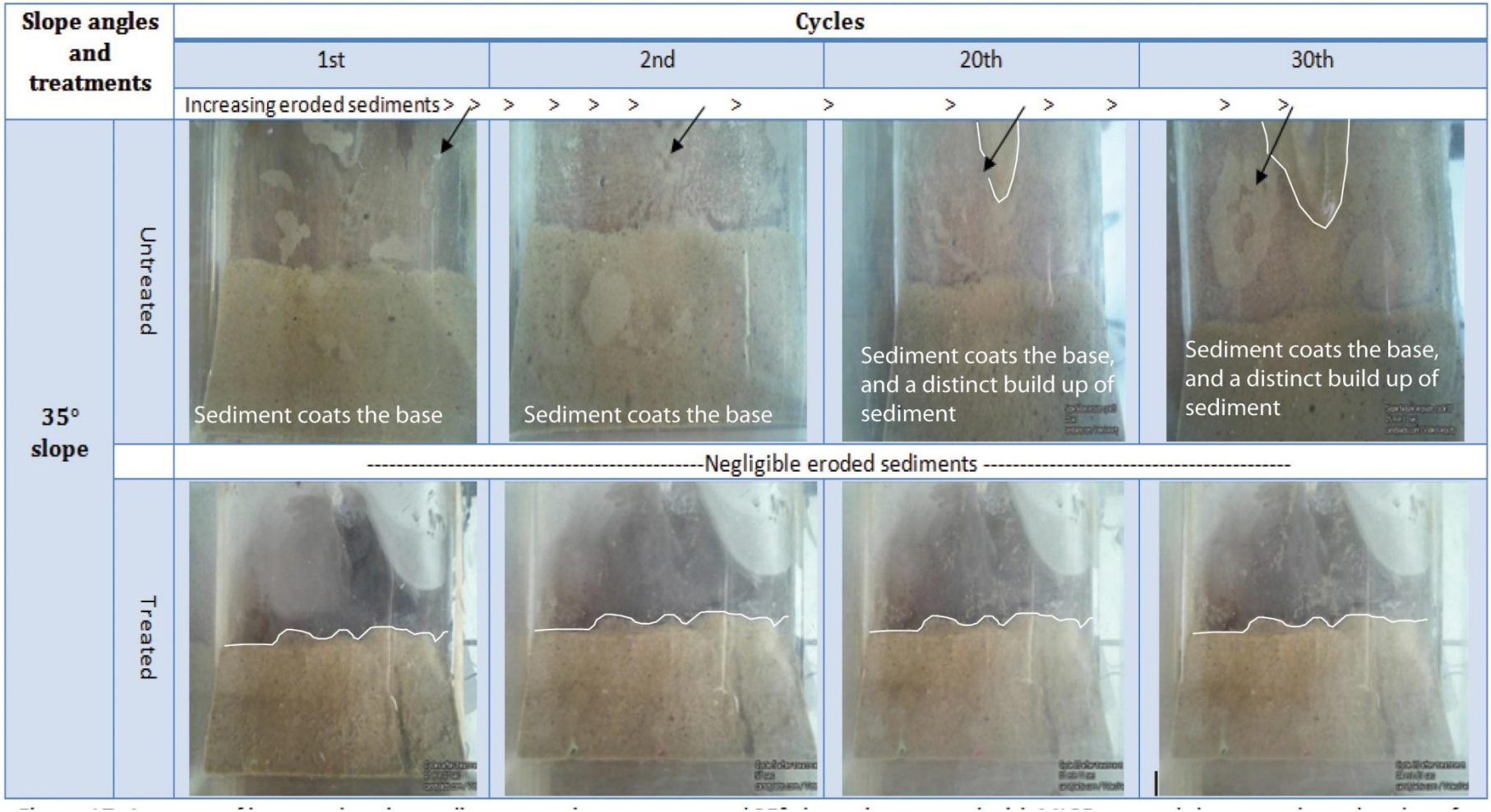

Figure 7. An array of images showing sediment erosion on untreated 35° slopes juxtaposed with MICP-treated slope at selected cycles of simulated tidal event. (white lines in untreated 20th and 30th cycles show build up of sediments at base of slope).

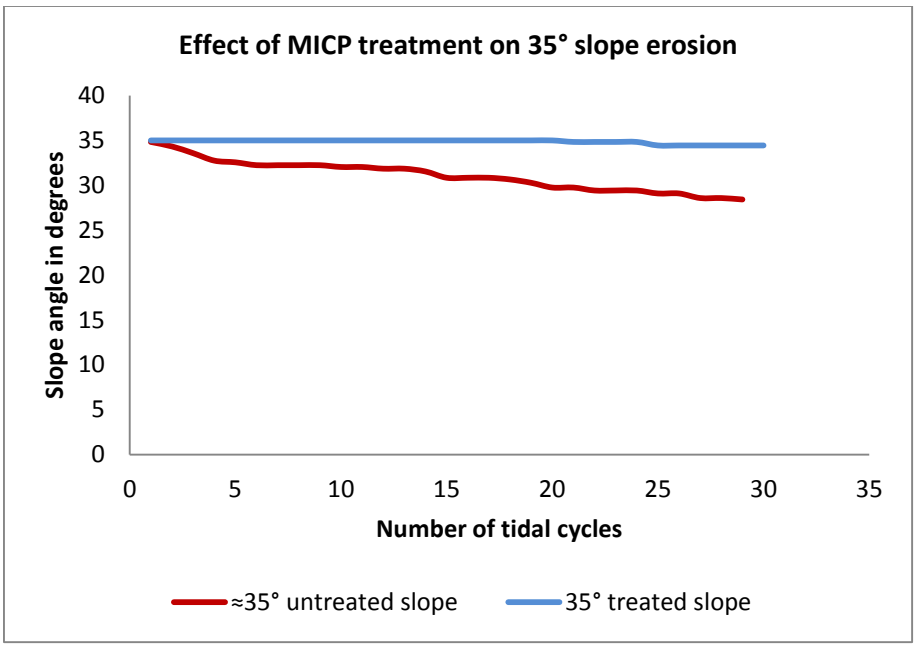

Figure 8: Graph comparing effect of MICP treatment on 35° slope erosion.

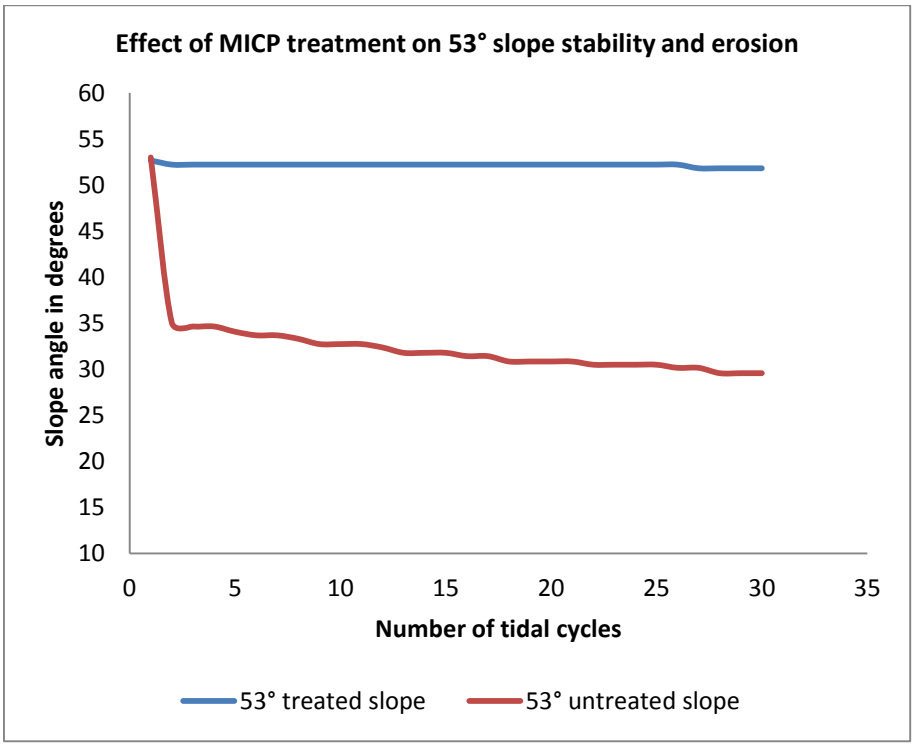

Figure 9: Graph comparing effect of MICP treatment on 53° slope erosion.

3.3 Assessment of effectiveness of treatments

Even though Section 3.2 and Figures 6-9 relatively show remarkable evidence of slope improvement, we looked at the various possible evidences of calcite formation (visual evidence, concentrations of effluent chemicals and mass balance after acid-washing of treated soils), and also performed unconfined compressive strength tests on cemented soil cores so as to roughly estimate its strength; these additional tests were meant to provide better understanding of the efficiency of the MICP treatments on the treated soil slopes. In principle, these tests could also serve as indicators of effective treatment in a field application. These are discussed in detail as follows:

Visual evidence of calcite formation.

Visual camera images showed a whitish fluid discharge from the foot of the slopes and staining the floor of the Perspex box; this became more evident after the third treatment cycle (see Fig. S2) and continued to increase in intensity in subsequent treatment cycles. White calcite patches became visible also on the soil slope surface. The slopes were very rigid and firm after treatment to the extent that it was difficult to detach the soil mass from the Perspex box.

Concentration of ammonium and calcium from treatment effluents.

Cation concentration in effluents, collected at foot of slope, provided an indication of MICP performance (Table 4). The production of ammonium, a by-product of ureolysis, indicated that the reactions for MICP were progressing. Ammonium fluctuations may be attributed to natural variability, since bacteria were grown on different days and three treatment cycles were performed per day. The S. pasteurii could have been at different metabolic activities during different cycles despite efforts to normalise procedures.

The reverse trend was apparent for the concentration of calcium. Calcite production occurred as reflected in the decreasing concentration of calcium in effluent; pore sizes may have reduced and

preferential nucleation of calcite on calcite (Tobler et al., 2011) may have also been the reason for this trend. Two pore volumes of 0.7 M $CaCl_2$ solution was injected into the soil per treatment cycle, leachate concentrations were between 0.14 M and 0.07 M calcium and suggest that most calcium was being retained in the soil.

Table 4: Ammonium and calcium concentrations (mol/L) in effluent collected after selected number of treatment cycles.

Sample concentration	Cycle 4	Cycle 7	Cycle 9	Cycle 11	Cycle 13
NH_4^+	0.044	0.046	0.12	0.038	0.11
Ca^{2+}	0.14	0.14	0.13	0.09	0.07

Mass balance after acid-washing of cemented soil

A third evidence of calcite precipitation, and hence soil cementation, was the result of mass reduction from acid digestion. The cemented soils were removed from the Perspex box, oven dried and weighed before and after acid (10% HCl) dissolution of calcites (Table 5). Adequate precautions were taken to ensure only negligible loss of sand due to flushing. Calcite production amounted to approximately 118-155 kg per m^3 of soil volume (or 4-5 mole $CaCO_3$ per litre of soil pore space). This was almost double the 60 kg calcite per m^3 of soil (or 2 mol $CaCO_3$ per litre of soil pore space) termed as highly effective for MICP according to Al Quabany, et al. (2012). The percentage of pore spaces filled by cementation material (13.0% and 9.9% for 35° and 53° slopes) was also high compared to the 6%-10%, deemed as the standard when stabilizing soils for other geotechnical

applications (Stavridakis, 2005; Mehmanavaz et al., 2012; Oti and Kinuthia, 2012). This work achieved double the level of efficiency expected for a typical MICP treatment in terms of calcite precipitated in a particular media. Also, MICP treatment resulted in slight reduction in the pore volume; hence cemented soil retained significant portion of porosity, which would be significant for future activities such as agriculture/vegetation on the sandy soil foreshore slope.

Table 5: Masses, volumes and amounts of calcite precipitated

Treated slope angle	35°	53°
Mass of calcites precipitated in soil during treatment (g)	51.9	55.3
Volume of calcite precipitated (cm^3)	19.2	20.4
% Soil pores filled by calcite precipitated	13.0	9.87
Amount of calcite produced (kg m^{-3} of soil)	155	118
Amount of calcite produced (mol L^{-1})	5.16	3.92

Assumptions (see Table S.2): dry density of sand, 1.49g cm^{-3}; soil porosity, 0.44; specific gravity of calcite, 2.71; 1 kg calcite per m^3 soil, (1/30) mol $CaCO_3$/litre of soil pore space (Al-Quabany, et al., 2012)

Strength of cemented soil

To get a rough estimate of the strength of cemented soil, four cylindrical cores were taken from the treated slopes (Figure S3) and subjected to unconfined compressive strength (UCS) test. It should be noted that the height to diameter ratio (1.2:1; with heights between 18 mm and 25 mm and diameters between 15mm and 30mm) obtained from the cemented soil slopes is lower than 2:1 required for

triaxial compression test due the size of the slopes in the microcosm. Nonetheless, uniaxial compressive strength recorded could be taken as an indication of the strength developed by the microbial-induced precipitation of calcite.

All samples tested failed at average stress of 470 (±3) kPa (Fig. S4). According to Collins and Sitar (2009), sands with unconfined compressive strength of between 100-400 kPa are categorised as moderately cemented, while below 100 kPa are weakly cemented sands. Going by this standard, therefore, the ability of the cemented sands in this work to withstand this level of stress implies that the MICP treatment achieved cementation above 'moderate' standards and with arguably homogeneous strength distribution across the media.

These additional tests and their results further buttress the outcomes represented in Figures 6-9; it has made explicit the fact that superlative amount of calcite was produced from the MICP process and these was sufficient enough to bring about a highly cemented soil slope capable of resisting collapse/failure and erosion under tidal current cycles.

4.0 Conclusions

Experimental microcosm demonstrated the mechanisms of slope failure and erosion obtainable on foreshore sandy soil slopes. Sediment detachment occurred and subsequent tidal cycles continued to erode the slope. After treatment with MICP, the treated slopes were visibly durable and filled up 9.9% of soil pores, which was almost double the benchmark for measuring MICP effectiveness (Al Quabany et al., 2012; Oti and Kinuthia, 2012). Furthermore, the cemented soils exhibited unconfined compressive shear strength classified as 'above moderate' (Collins and Sitar, 2009). MICP treated soils were significantly more improved compared to untreated one subjected to the same thirty tidal current cycles to check stability and erosion.

Erosion and slope stabilization issues are diverse and occur in varied locations/conditions. The technique applied in this study for sandy soil stabilization and erosion mitigation have also shown remarkable success in field trials aimed at ground reinforcement (van Paassen et al., 2009), however, one of the greatest challenges in field trials experimented so far has been the non-heterogeneous distribution or penetration of treatment across soil volumes; perhaps this may be due to insufficient consideration of the limitations posed by boundary effects and other related factors when up-scaling from laboratory based microcosms to field trials. These crucial aspects ought to be adequately addressed if the objective is to modify strength and permeability uniformly across relatively large volumes of soils. For protection from erosion and stabilization of an embankment's slope, a relatively shallow penetration of treatment (10 - 20cm), would be sufficient; this should be easy to achieve considering methodologies already experimented, with relative success, in the field.

Acknowledgements

The authors thank James Minto for proof reading; Mara Knapp, John Carlin, Derek McNee for helping out with supplies at the labs in University of Strathclyde. The project was funded with Department of Civil & Environmental Engineering laboratory budgets, and authors declare no competing financial interests.

References

Agassi, M. and Ben, H.M. (1992). Stabilizing steep slopes with soil conditioners and plants. Soil Technol. 5 (3): 249–256.

Al Quabany, A., Soga, K., and Santamarina, C. (2012) Factors affecting efficiency of microbially induced calcite precipitation. J. Geotech. Geoenviron. Eng. 138 (8): 992–1001.

Amos, C.L., Brylinski, M., Lee, S., and O'Brien, D., (1996) Littoral mudflat stability monitoring, the Number estuary, S. Yorkshire., England. USPIJK, April 1995. Geological Survey of Canada Open file report no. 3214.

ASTM. (2004). Test specification for unconfined compressive strength of cohesive soil, D2166-00, ASTM International, West Conshohocken, Pa.

ASTM. (2006). Standard Practice for Classification of Soils for Engineering Purposes (Unified Soil Classification System), D2487-06e1. ASTM International, West Conshohocken, PA.

ASTM. (2007). Standard method for particle-size analysis of soils, D422-63e2. ASTM International, West Conshohocken, PA.

Collins, B. D., and Sitar, N. (2009) Geotechnical properties of cemented sands in steep slopes. J. Geotech. Geoenviron. Eng. 135(10):1359–1366.

Conley, D.C. and Griffin J.G. (2004) Direct measurements of bed stress under swash in the field. J. Geophys. Res. 109:C03050 http://dx.doi.org/10.1029/2003JC001899.

Conley, D.C. and Inman D.L. (1994) Ventilated oscillatory boundary layers. J. Fluid Mech. 273: 262–284

1 Cowen, E.A., Sonu, I.M., Liu, P.L.F., and Raubenheimer, B. (2003) 'Particle image velocimetry
2 measurements within a laboratory-generated swash zone'. J. Eng. Mech. 129: 1119–1129.

3 Cox, D.T., Hobensack, W., and Sukumaran, A. (1998) 'Bottom stress in the inner surf and swash
4 zone'. Proceedings of the 27th International Conference on Coastal Engineering, ASCE: 108–119.

5 Dejong, J.T., Soga, K., Kavazanj, I.E., Burns S., Van Paassen, L.A., Al Qabany, A., Aydilek, A.,
6 Bang, S.S., Burbank, M., Caslake, L.F., Chen, C.Y., Cheng, X., Chu, J., Ciurli, S., Esnault-Filet, A.,
7 Fauriel, S., Hamdan, N., Hata, T., Inagaki, Y., Jefferis, S., Kuo, M., Laloui, L., Larrahondo, J.,
8 Manning, D.A.C., Martinez, B., Montoya, B.M., Nelson, D.C., Palomino, A., Renforth, P.,
9 Santamarina J.C., Seagren, E.A., Tanyu, B., Tsesarsky, M., and Weaver, T. (2013) Biogeochemical
10 processes and geotechnical applications: progress, opportunities and challenges. Geotechnique
11 63(4): 287–301.

12 DeJong, J.T., Fritzges, M.B., Nusslein, K. (2006) Microbial induced cementation to control sand
13 response to undrained shear. J. Geotech. Geoenv. Engrg, ASCE. 132(11): 1381–1392.

14 DeJong, J.T., Martinez, B.C., Mortensen, B.M., Nelson, D.C., Waller, J.T., Weil, M.H., Ginn, T.R.,
15 Weathers, T., Barkouki, T., Fujita, Y., Redden, G., Hunt, C., Major, D., and Tanyu, B. (2009)
16 Upscaling of bio-mediates soil improvement. Proceedings of the 17th International Conference on
17 Soil Mechanics and Geotechnical Engineering, Alexandria, Egypt.

18 El Mountassir, G., Lunn, R., Moir, H., and MacLachlan, E.C. (2014) Hydrodynamic coupling in
19 microbially mediated fracture mineralization: formation of self-organized groundwater flow
20 channels. Water Resources Res. 50: 1-16.

21 Elfrink, B. and Baldock, T. (2002) Hydrodynamics and sediment transport in the swash zone: a
22 review and perspectives. Coast. Eng. 45: 149–167.

1 Esnault-Filet, A., Gadret, J.P., Loygue, M. and Borel, S. (2012) Biocalcis and its application for the
2 consolidation of sands. In: Johnsen, L. F., Bruce, D. A. and M. J. Byle (eds.), Grouting and deep
3 mixing. Geotechnical Special Publication 288. Reston, VA, USA: ASCE. Vol. 2, pp. 1767–1780.

4 Fang, H.W. and Wang, G.Q. (2000) Three-dimensional mathematical model for suspended sediment
5 transport. J. Hydraul. Eng., ASCE. 126(8): 578–592.

6 Fang., N.F., Shi, Z.H., Yue, B.J., and Wang, L. (2013) The characteristics of extreme erosion events
7 in a small mountainous watershed. PLoS One 8(10): e76610.

8 Ferris, F.G., Stehmeier, L.G., Kantzas, A., and Mourits, F.M. (1996) Bacteriogenic mineral
9 plugging. J. Can. Petr. Technol. 35 (8): 56–61.

10 Fujii, T., and Raffaelli, D. (2008) Sea-level rise, expected environmental changes, and responses of
11 intertidal benthic macrofauna in the Humber estuary, UK. Mar. Ecol. Prog. Ser. 371: 23–35.

12 Haller, M.C., Honegger, D., and Catalan, P.A. (2014) Rip current observations via marine radar. J.
13 Waterway, Port, Coastal, Ocean Eng. 140: 115-124.

14 Harkes, M.P., Booster, J.L., van Paassen, L.A., van Loosdrecht, M.C.M. (2008) Microbial induced
15 carbonate precipitation as ground improvement method –bacterial fixation and empirical correlation
16 $CaCO_3$ vs. strength. 1st International Conference on Bio-Geo-Civil Engineering, Netherlands; June
17 23- 25. pp. 37–41.

18 Harkes, M.P., van Paassen, L.A., Booster, J.L., Whiffin, V.S., and van Loosdrecht, M.C.M. (2010)
19 Fixation and distribution of bacterial activity in sand to induce carbonate precipitation for ground
20 reinforcement. Ecol. Eng. 36: 112–117.

1 Ivanov, V., and Chu, J. (2008) Applications of microorganisms to geotechnical engineering for
2 bioclogging and biocementation of soil in situ. Rev. Environ. Sci. Biotechnol. 7: 139–153.

3 Liu, D., and Li, Y. (2003) Mechanism of plant roots improving resistance of soil to concentrated
4 flow erosion. J. Soil Water Conserv. 17(3): 34–37.
5 Liu, J., Shi, B., Huang, H., and Jiang, J. (2009) Improvement of water-stability of clay aggregates
6 admixed with aqueous polymer soil stabilizers. Catena. 77: 175–179.

7 Liu, J., Shi, B., Jiang, H., Huang, H., Wang, G., and Kamai, T. (2011) Research on the stabilization
8 treatment of clay slope topsoil by organic polymer soil stabilizer. Eng. Geol. 117: 114-120.

9 Longo, S., Petti, M., and Losada, I.J. (2002) Turbulence in the swash and surf zones: a review.
10 Coast. Eng. 45: 129-147.

11 MacMahan, J., Thornton, E.B., and Reniers, A.J.H.M. (2006) Rip current review. J. Coast. Eng. 53
12 (2-3): 191 - 208.

13 Masselink, G., Evans, D., Hughes, M.G., and Russell, P. (2005) Suspended sediment transport in the
14 swash zone of a dissipative beach. Mar. Geol. 216 (3): 169-189.

15 Mehmannavaz, T., Bhutta, M.A.R., Sumadi, S.R., and Sajjadi, M. (2012) Stabilization of desert sand
16 in Iran using cement and microsilice. AES-ATEMA Tenth International Conference on Advances and
17 Trends in Engineering Materials and their Applications. Montreal, Canada: June 18 – 22.

18 Mitchell, J.K., and Santamarina, J.C. (2005) Biological considerations in geotechnical engineering.
19 J. Geotech. Geoenviron. Eng. ASCE. 131(10): 1222–1233.

20 Mitchell, A.C., Dideriksen, K., Spangler, L.H., Cunningham, A.B., and Gerlach, R. (2010)
21 Microbially enhanced carbon capture and storage by mineral-trapping and solubility-trapping.
22 Environ. Sci. Technol. 44: 5270 - 5276. Doi 10.1021/es903270w.

1 Miura, K., Maeda, K., and Shosuke, T. (1997) Method of measurement for the angle of repose of
2 sand. Soils Foundat. 37(2): 89-96.

3 Oti, J.E., and Kinuthia, J. M. (2012) Stabilised unfired clay bricks for environmental and sustainable
4 use. Appl. Clay Sci. 58: 52-59.

5 Petti, M., and Longo, S. (2001) Turbulence experiments in the swash zone. Coast. Eng. 43: 1–24.

6 Scot, T., Russell, P., Masselink, G., and Wooler, A. (2009) Rip current variability and hazard along
7 a macro-tidal coast. J. Coast. Res. Special issue 56: 895-899.

8 Sharples, C., (2006) Indicative Mapping of Tasmanian Coastal Vulnerability to Climate Change
9 and Sea-Level Rise: Explanatory Report (Second Edition); Consultant Report to Department of
10 Primary Industries & Water, Tasmania.

11 Short, A.D. and Brander, R. (1999) Regional variation in rip density. J. Coast. Res. 15: 813-822.

12 Short, A.D. (1985) Rip current type, spacing and persistence, Narrabeen beach, Australia. Mar.
13 Geol. 65: 47–71.

14 Singh, A. K. (2010) 'Bioengineering techniques of slope stabilization and landslide
15 mitigation. Disaster Prevention and Management. 19**,** pp. 384-397.

16 Stavridakis, E.I. (2005) Evaluation of engineering and cement–stabilization parameters of clayey–
17 sand mixtures under soaked conditions. Geotech. Geol. Eng. 23: 635–655.

18 Tobler, D. J., Cuthbert, M. O., Greswell, R. B., Riley, M. S., Renshaw, J. C., Handley- Sidhu, S.
19 and Phoenix, V. R. (2011) 'Comparison of Rates of Ureolysis between Sporosarcina pasteurii and
20 an Indigenous Groundwater Community under Conditions Required to Precipitate Large Volumes
21 of Calcite'. Geochim. Cosmochim. Acta, 75**:**3290–3301.

1 Uzunoglu, E., Bicer, A.Z.Y., Dolapci, I. and Dogan, A. (2014) Biofilm-forming ability and
2 adherence to poly-(methyl-methacrylate) acrylic resin materials of oral Candida albicans strains
3 isolated from HIV positive subjects. J. Adv. Prosthodont. 6(1): 30–34.

4 Van Paassen, L.A., Harkes, M.P., Van Zwieten, G.A., Van der Zon, W.H., Van der Star, W.R.L. and
5 Van Loosdrecht, M.C.M. (2009) Scale up of BioGrout: a biological ground reinforcement method.
6 Proceedings of 17th International Conference of Soil Mechanical and Geotechnical Engineering,
7 Alexandria, Egypt pp. 2328–2333.

8 Van Paassen, L.A., Ghose, R., van der Linden, T.J.M., van der Star, W.R.L., and van Loosdrecht,
9 M.C.M. (2010) Quantifying biomediated ground improvement by ureolysis: large-scale biogrout
10 experiment. ASCE J. Geotech. Geoenviron. Eng. 136: 1721–1728.

11 Van Paassen, L.A., Whiffin, V.S. and Harkes, M.P. (2007) Immobilization of bacteria to a
12 geological material. Netherlands Patent assignee Stichting GeoDelft. EP1798284-A1;
13 WO2007069884-A1.

14 Whiffin V.S., Van Paassen, L.A., and Harkes, M.P. (2007) Microbial carbonate precipitation as a
15 soil improvement technique. Geomicrobiol. J. 24(5): 417–423.

16 Winn, P.J.S., Young, R.M., and Edwards, A.M.C. (2003) Planning for the rising tides: the Humber
17 Estuary Shoreline Management Plan. Sci. Tot. Environ. 314–316: 13–30.
18

Supplemental Information

Application of microbially induced calcite precipitation in erosion mitigation and stabilization of sandy soil foreshore slopes

Emmanuel Salifu [a,c], Erica MacLachlan [a], Kaanan Iyer [a,b], Charles W. Knapp [a], Alessandro Tarantino [a]

[a] Department of Civil & Environmental Engineering, University of Strathclyde, Glasgow, UK

[b] Department of Civil Engineering, Indian Institute of Technology-Bombay, Mumbai, India

Supplemental figures:

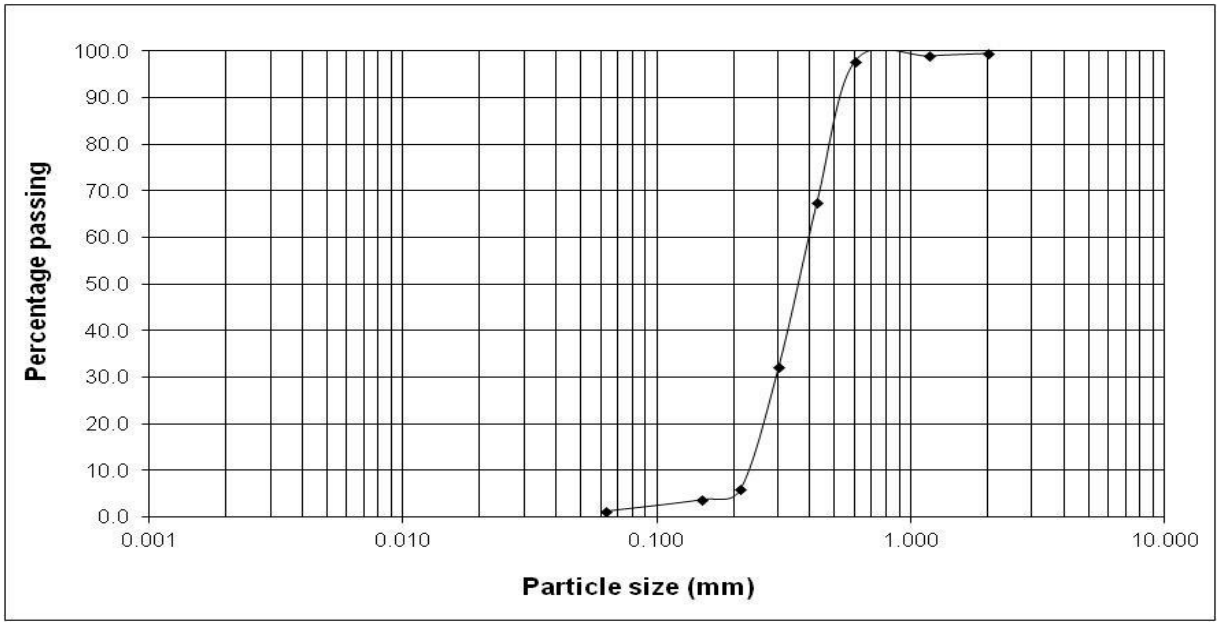

Figure S1: Grain size distribution curve representing the sand used in the experiments. Sand was collected from Troon beach, Ayrshire, U.K.

1

	Before treatment	At 3rd treatment cycle	At 18th treatment cycle
35°			
53°			

2

3

4

Figure S2: Visual evidence of calcite precipitation as treatment progressed. Arrows show whitish fluid on floor of Perspex box; see also the white patches on soil surface.

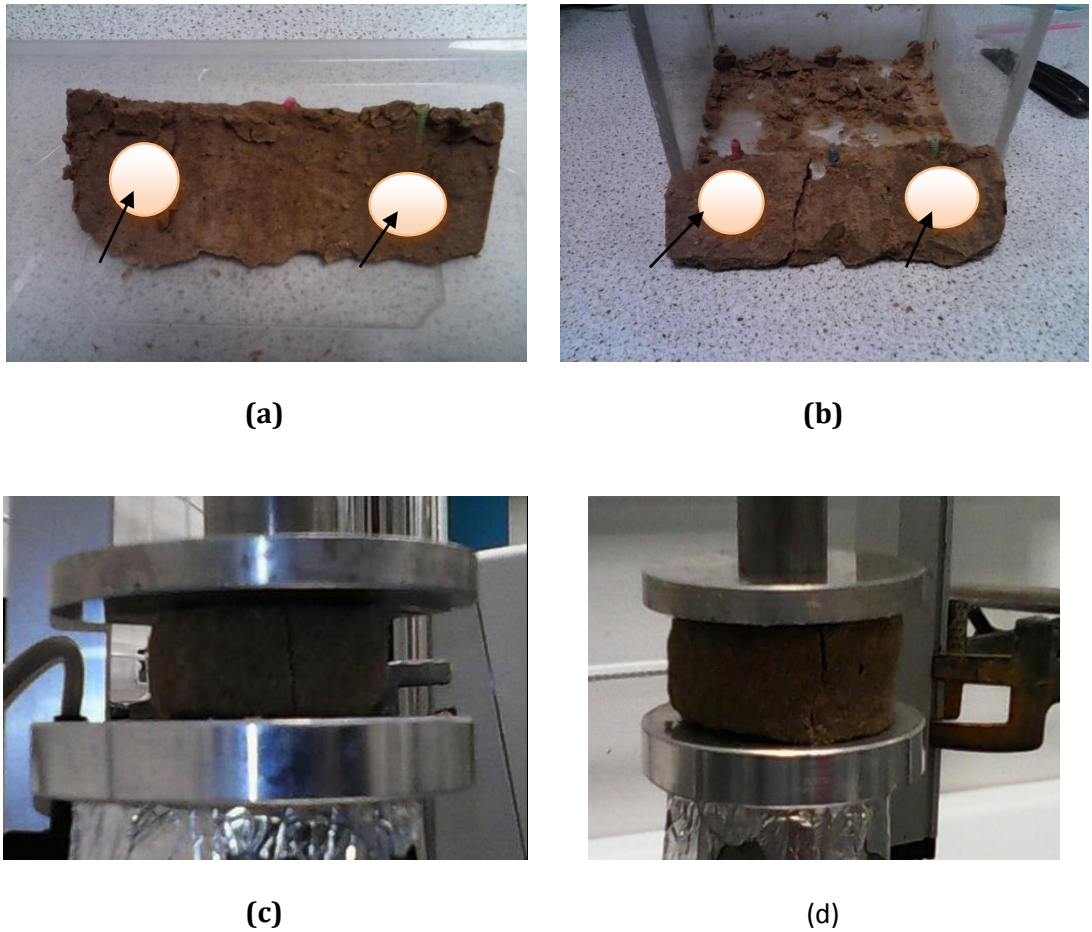

(a) **(b)**

(c) (d)

Figure 3: (a and b) core sampling points and (c and d) failed cores under UCS testing machine.

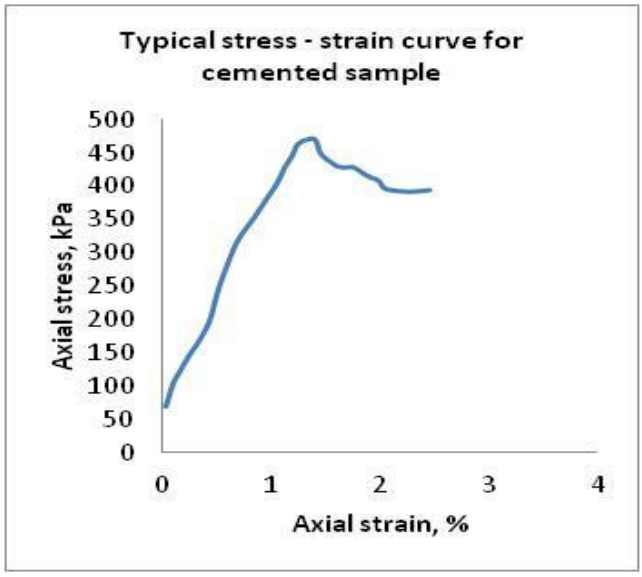

Figure S4: A typical stress-strain graph of the samples subjected to UCS test.

Supplemental tables

Table S.1: Constituents of Blood Heart Infusion (BHI) agar and BHI broth

Media	Components	Mass proportion (gL^{-1} of distilled water)
BHI agar	Brain Heart, Infusion from (solids)	8.0
	Dextrose	2.0
	Peptic Digest of Animal Tissue	5.0
	Disodium Phosphate	2.5
	Pancreatic Digest of Casein	16.0
	Agar	13.5
	Sodium Chloride	5.0
BHI broth	beef heart (infusion from 250g)	5.0
	calf brains (infusion from 200g)	12.5
	disodium hydrogen phosphate	2.5
	D(+)-glucose	2.0
	peptone	10.0
	sodium chloride	5.0

Table S.2: Masses, volumes and amounts of calcite precipitated.

	Treated slope angle	35°	53°
a	Mass of oven-dried soil before treatment (g)	500	700
b	Volume of soil treated (cm^3) [(a/1.49 g cm^{-3}*)]	335.57	469.80
c	Pore volume of dry soil treated (cm^3) [(b x 0.44**]	147.65	206.71
d	Mass of oven-dried cemented soil at end of treatment (g)	541.00	754.75
e	Mass of oven-dried soil after acid washing (g)	489.07	699.45
f	Mass of calcites precipitated in soil during treatment (g) [d - e]	51.93	55.30
g	Volume of calcite precipitated (cm^3) [f/2.71***]	19.16	20.41
h	% Soil pores filled by calcite precipitated [(g/c) x 100]	12.98	9.87
i	Amount of calcite produced kg m^{-3} of soil [f/b x 1000]	154.75	117.70
j	Amount of calcite produced Mol L^{-1} [i x (1/30)***]	5.16	3.92

*Dry density of sand = 1.49g cm^{-3}; **Soil porosity = 0.44; *** Specific gravity of calcite = 2.71; ****1 kg calcite per m^3 soil = (1/30) mol $CaCO_3$ per litre of soil pore space (Al-Quabany et al, 2012)